Supplementary information

A Novel Ketogenesis-Integrated Model of Fat and Carbohydrate Oxidation

Nguyen A.[1,2,3⊕], Osorio Perez, O. [1,2,3⊕], Jackemeyer D. [2,3⊕], Terrera M.[2,3,4,5⊕], Pradhan A. [1,2,3], Chen, F.[2], Hua Y.,[6] Chou, C.[6], Cheng, S.[6]*, Forzani, E. [1,2,3]*

⊕*Equal contributions' authors*

[1] School of Engineering for Matter, Transport and Energy, Arizona State University, Tempe, AZ 85287, U.S.A.
[2] Center for Bioelectronics and Biosensors, Biodesign Institute, Arizona State University, 1001 S McAllister Ave., Tempe, AZ 85281, U.S.A.
[3] Medical Devices and Methods Laboratory, Health Futures Center, Arizona State University, 6161 E. Mayo Blvd., Phoenix, Az 85054, U.S.A.
[4] Universidad Provincial de Cordoba, Cordoba, 5000, Argentina.
[5] Universidad Nacional de Cordoba, Ciudad Universitaria, Cordoba, 5000, Argentina.
[6] Amazon,

* Correspondence: chengs@lab126.com (S.C.), eforzani@asu.edu (E.F.)

1. Intrasubject Study of Skin Acetone Excretion Rate

In this work we have successfully developed the first ketogenesis-integrated model of fat and carb oxidation. We have found the model fat oxidation rate to be directly proportional to breath and skin acetone. In this supplementary information section, we explore more in detail how fat oxidation correlates with breath and skin acetone for individual subjects (Figure S1).

Correlation plots between fat oxidation and breath/skin acetone

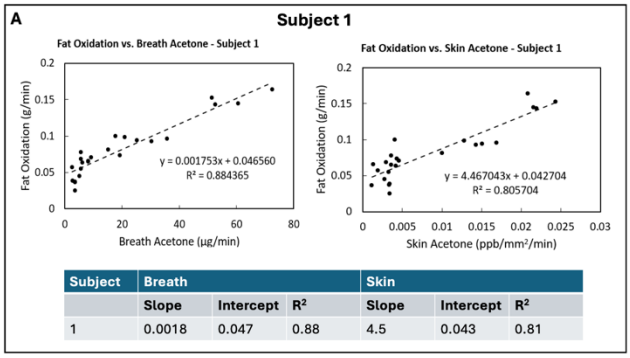

Subject	Breath			Skin		
	Slope	Intercept	R^2	Slope	Intercept	R^2
1	0.0018	0.047	0.88	4.5	0.043	0.81

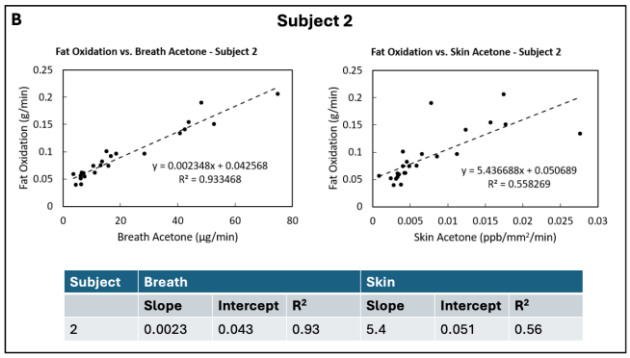

Subject	Breath			Skin		
	Slope	Intercept	R^2	Slope	Intercept	R^2
2	0.0023	0.043	0.93	5.4	0.051	0.56

C

Subject 3

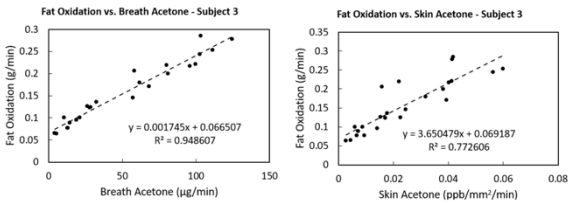

Subject	Breath			Skin		
	Slope	Intercept	R^2	Slope	Intercept	R^2
3	0.0017	0.067	0.95	3.7	0.069	0.77

D

Subject 4

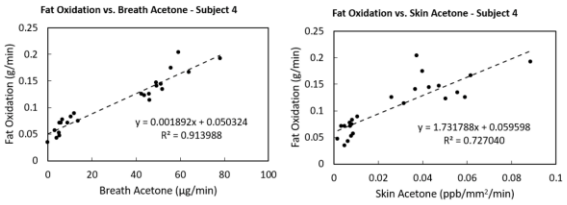

Subject	Breath			Skin		
	Slope	Intercept	R^2	Slope	Intercept	R^2
4	0.0019	0.050	0.92	1.7	0.060	0.73

E

Subject 5

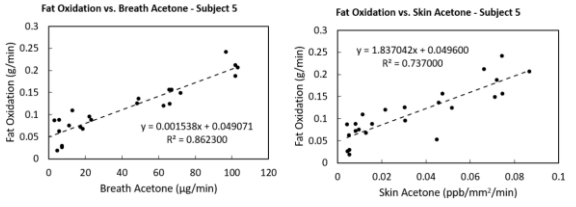

Subject	Breath			Skin		
	Slope	Intercept	R^2	Slope	Intercept	R^2
5	0.0015	0.049	0.86	1.8	0.050	0.74

F

Subject 6

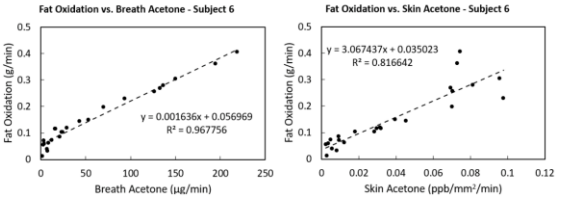

Subject	Breath			Skin		
	Slope	Intercept	R^2	Slope	Intercept	R^2
6	0.0016	0.057	0.97	3.1	0.035	0.82

G

Subject 7

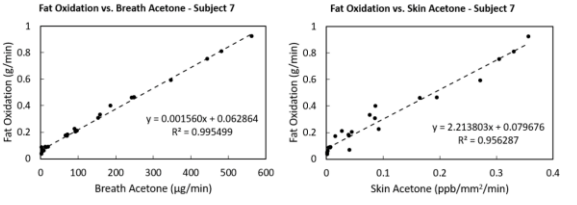

Subject	Breath			Skin		
	Slope	Intercept	R^2	Slope	Intercept	R^2
7	0.0016	0.063	1.0	2.2	0.080	0.96

H

Subject 8

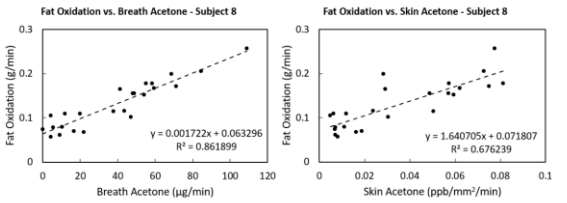

Subject	Breath			Skin		
	Slope	Intercept	R^2	Slope	Intercept	R^2
8	0.0017	0.063	0.86	1.6	0.072	0.68

I

Subject 9

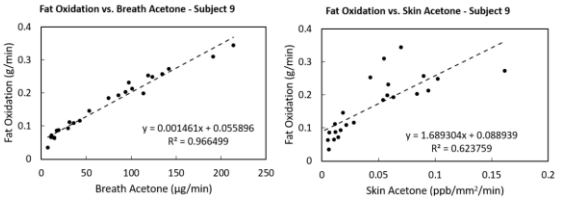

Subject	Breath			Skin		
	Slope	Intercept	R^2	Slope	Intercept	R^2
9	0.0015	0.056	0.97	1.7	0.089	0.62

J

Subject 10

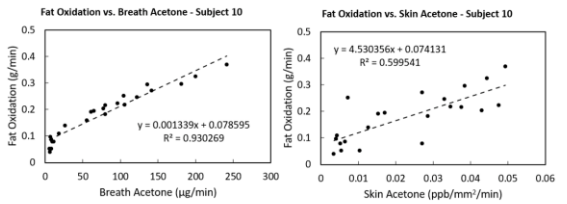

Subject	Breath			Skin		
	Slope	Intercept	R^2	Slope	Intercept	R^2
10	0.0013	0.079	0.93	4.5	0.074	0.60

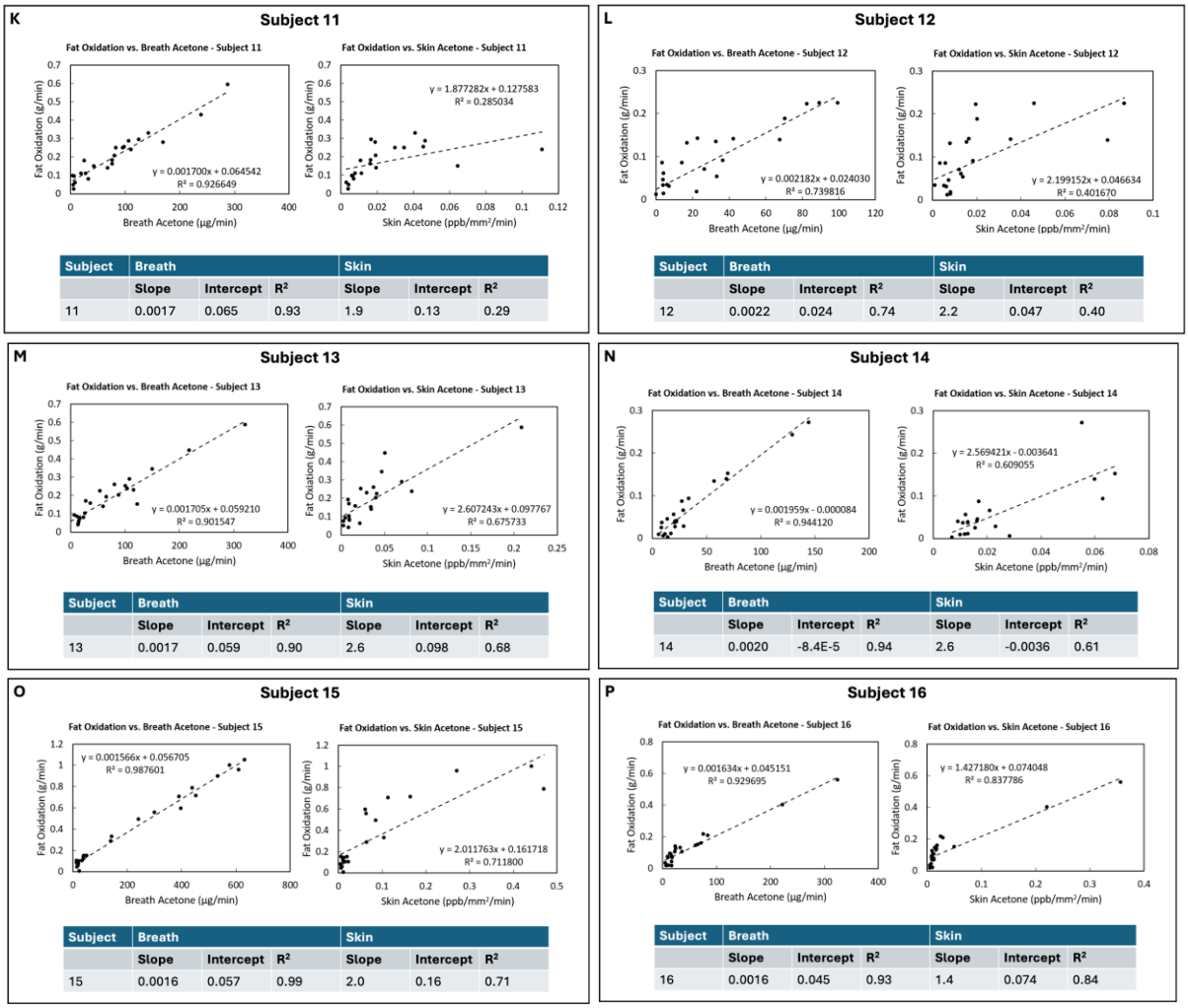

Figure S1. Correlation plot between fat oxidation and (left) breath acetone; and (right) skin acetone for each subject from (A) to (P).

As seen in figure S1, the fat oxidation correlates well with the breath acetone for most of the subjects with regression coefficients (R^2) of 0.7 - 0.9.

In comparison to breath acetone, we observe that the correlation between fat oxidation rate and skin acetone excretion rate shows subjects (1, 6, 7, and 16) with a strong correlation ($R^2 > 0.8$), while subjects (2, 11, 12) exhibit a lower correlation, potentially due to an unstill condition during sample collection. This highlights the importance of proper sealing conditions for

accurate skin acetone collection. Furthermore, there is an overall good regression correlation between fat oxidation from the model (R^2 = 0.6 - 0.8) for the majority of the remaining subjects (3, 4, 5, 8, 9, 10, 13, 14 and 15).

2. Comparing all subjects in the same intervention week

Figure S2 shows the trend of fat and carb oxidation of 16 subjects in the same intervention week.

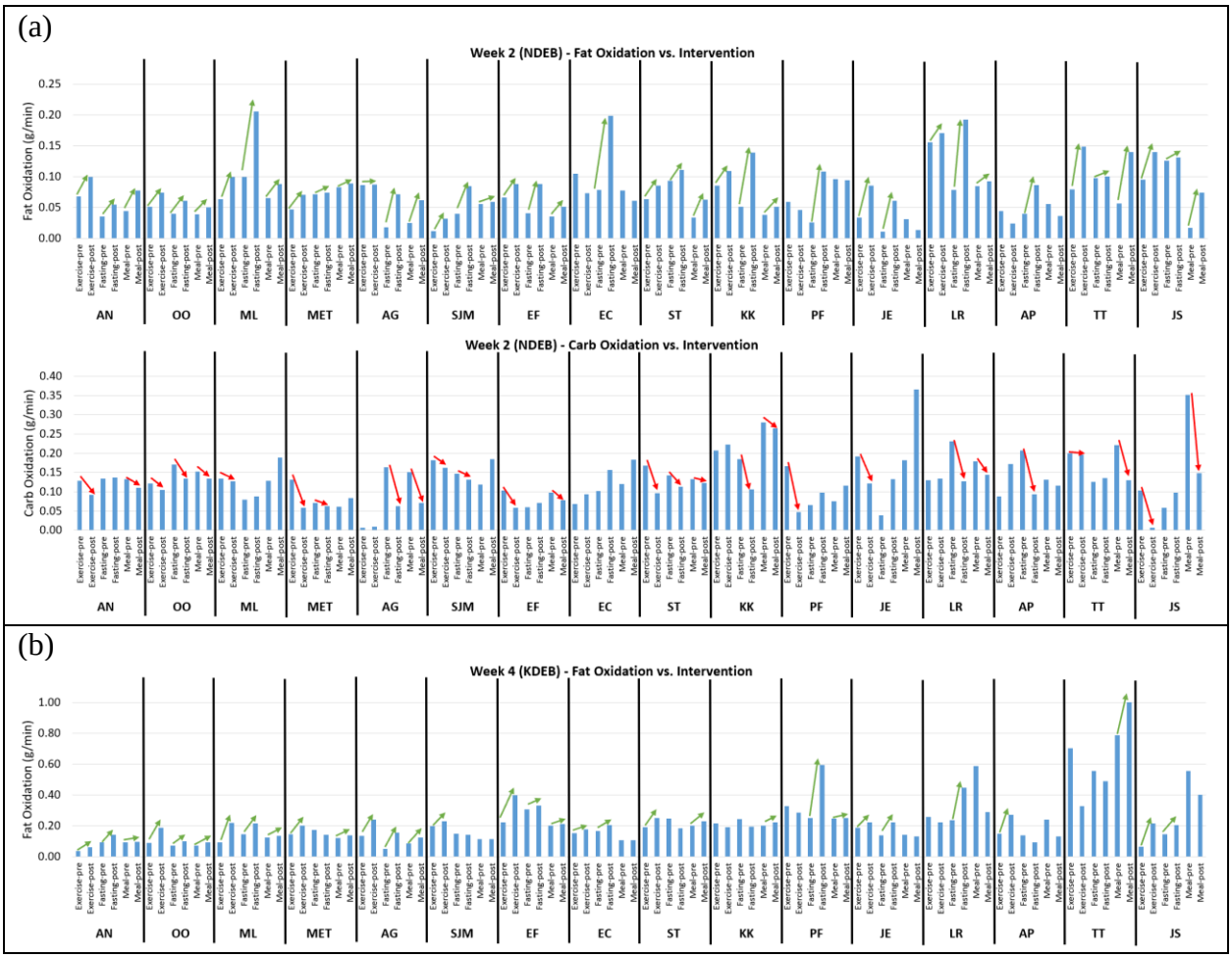

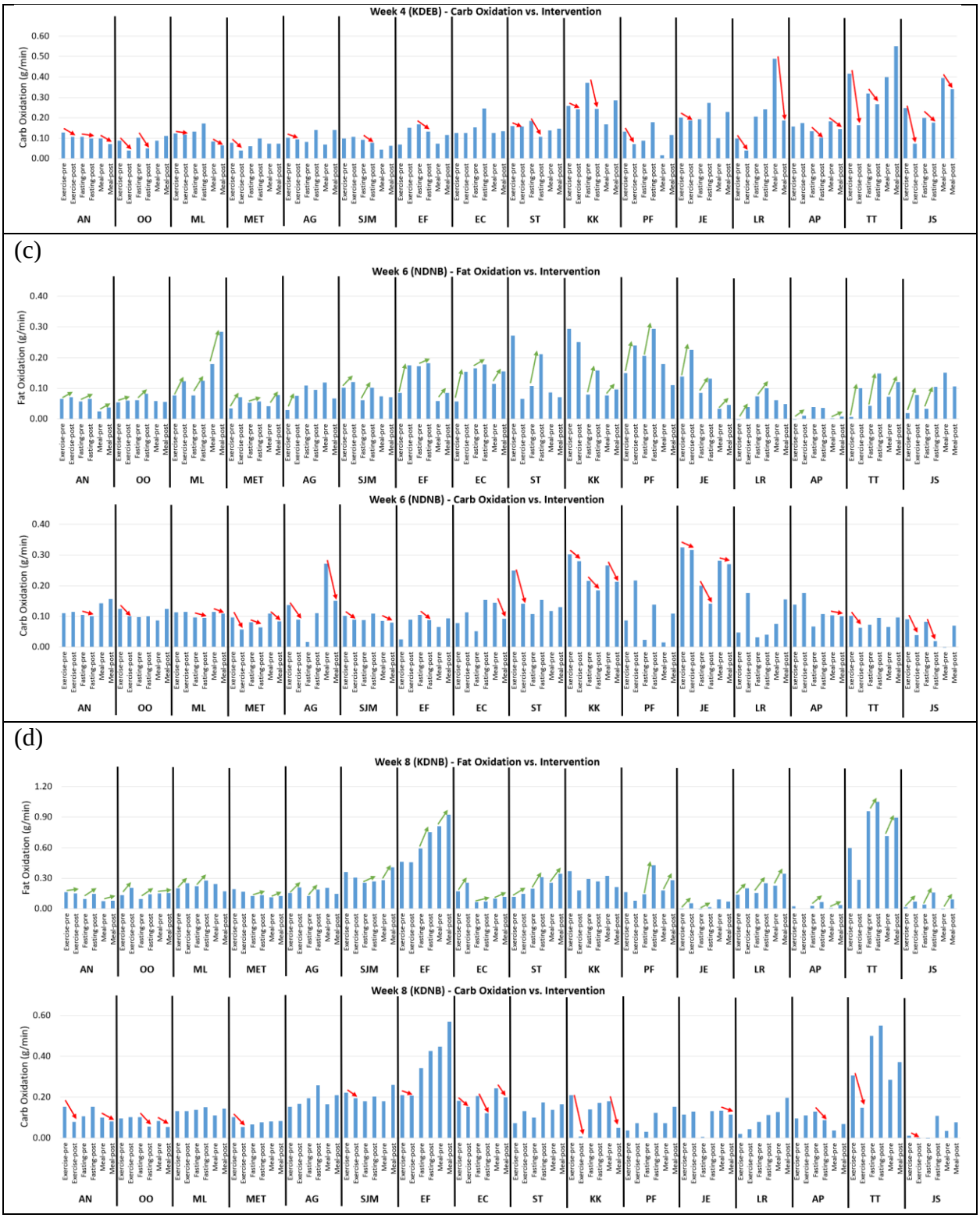

Figure S2. Fat and carb oxidation trends for each subject in week (a) 2; (b) 4; (c) 6; and (d) 8.

Table S1. Summary of fat and carb oxidation trend for each week

Week	Increase in Fat oxidation (%)	Decrease in Carb oxidation (%)
2	85.4	58.3
4	66.7	54.2
6	77.1	50.0
8	75.0	33.3

As seen in figure S2 and table S1, based on the data obtained for pre and post measurements, most subjects show the increase in fat oxidation as expected from the interventions applied on the subjects. The increase in fat oxidation is correlated with decreases in carb oxidation, primarily during normal diet/ energy balance (NDEB) and keto diet/ energy balance (KDEB). However, as discussed in the main manuscript, the number of cases where carb oxidation decreased was reduced as the study transitioned to Negative Energy Balance (NEB) weeks (4, and 6), especially when high ketosis occurs.

3. Comparing all subjects in between intervention weeks.

Figure S3 compares the absolute fat oxidation rate average of all subjects for same diet and same energy balance in between intervention weeks:

Figure S3a: EB: W2 (ND) vs. W4 (KD)

Figure S3b: NEB: W4 (ND) vs. W8 (KD)

Figure S3c: ND: W2 (EB) vs. W6 (NEB)

Figure S3d: KD: W4 (EB) vs. W8 (NEB)

Figure S3. Fat oxidation of each subject for (a) EB; (b) NEB; (c) ND; and (d) KD.

4. Model Quality Assurance and Validation

Model Quality Assurance with another set of subjects

In a separate study, we had 6 subjects undergo 2-day intervention, with the first day in a low ketosis condition and the second day in a high ketosis condition. The same experimental method was used. The developed fat calculation model was applied in this study for quality assurance of the results. Figures S4, S5 and S6 show the corresponding data for this separate study, including ketone contributions, fat oxidation rate calculated from the new ketogenesis-integrative model, and correlations of the model calculation with biomarkers of breath and skin acetone, respectively.

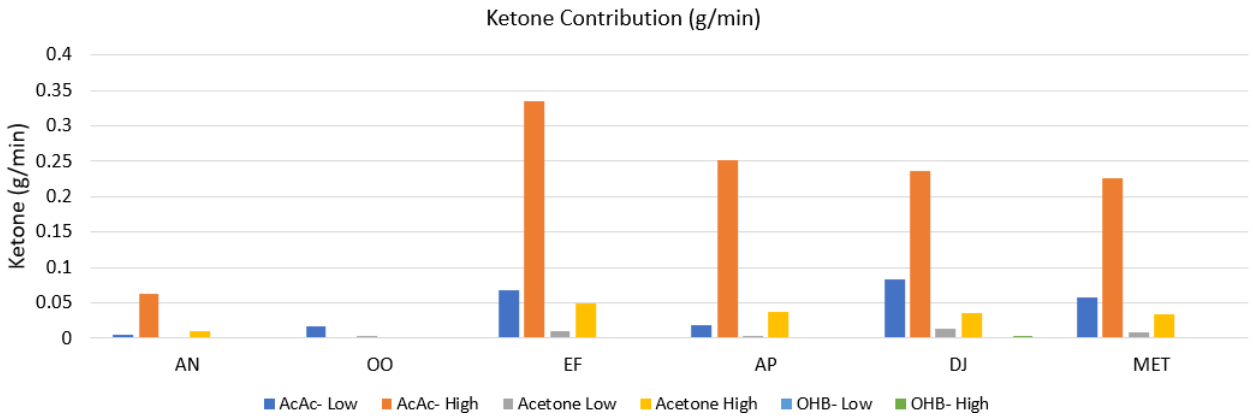

Figure S4. Ketone contribution in high and low ketosis for every subject.

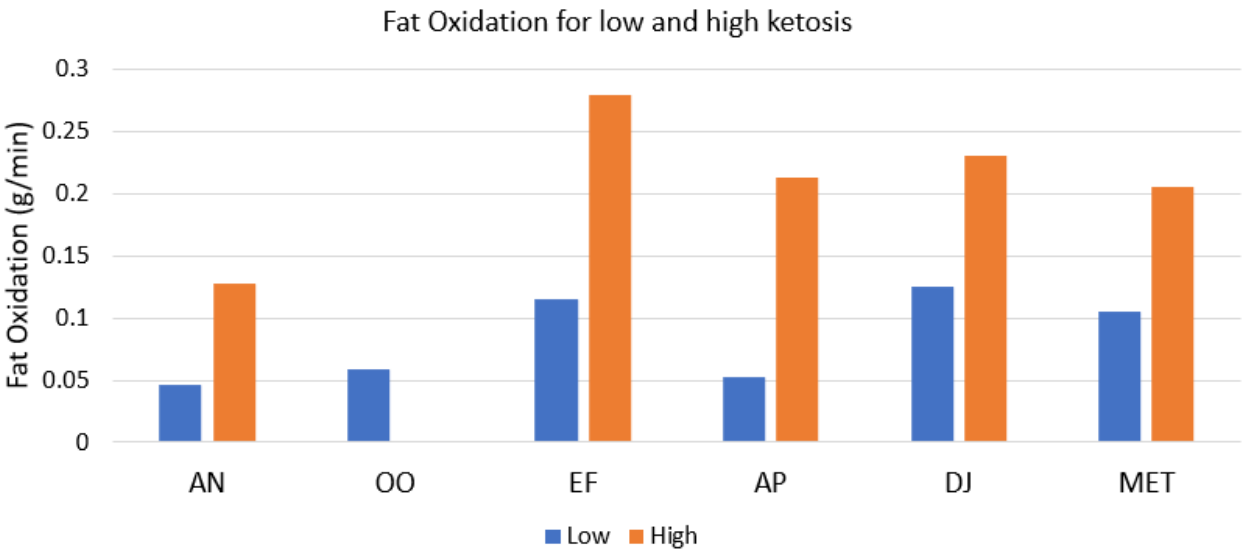

Figure S5. Fat oxidation in high and low ketosis for every subject.

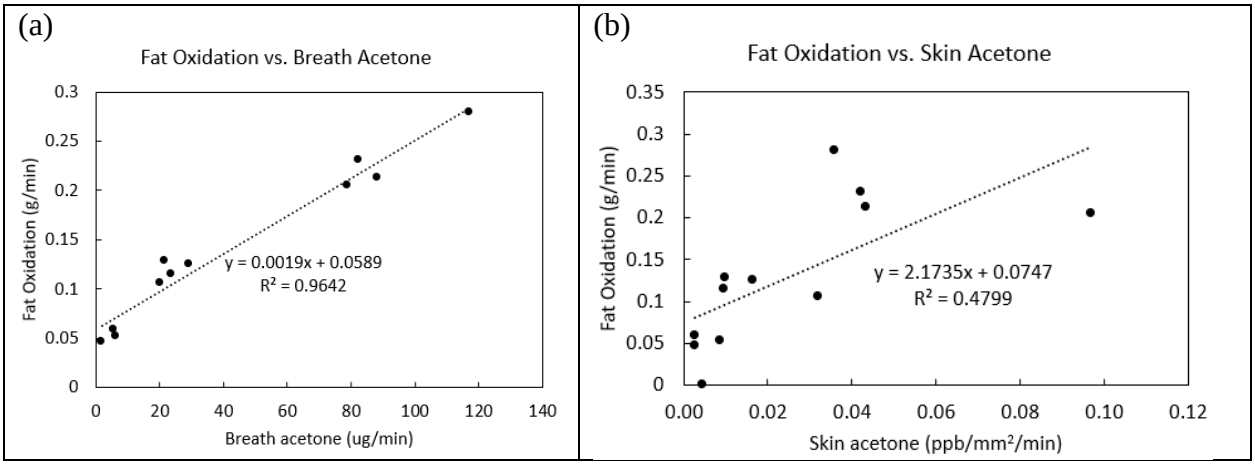

Figure S6. Correlation between fat oxidation and (a) breath acetone; and (b) skin acetone.

The data from this study were superimposed with the previous study (main manuscript data) and correlated with the predicted fat model (Figures S7 and S8). The correlation plots (Figures S7b and S8b) rendered slopes close to 1. Both the good level of overlapping of data (Figure S7a and S8a) and the correlation slopes (Figure S7b and S8b) indicated an excellent Quality Assurance of the study's methodology and data assessment.

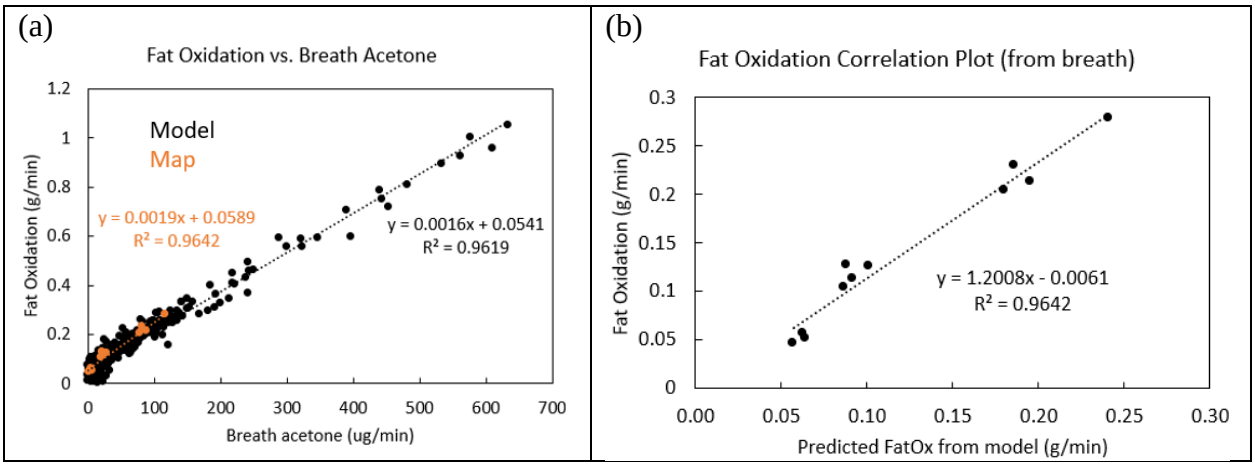

Figure S7. (a) Overlapping of the two correlations between fat oxidation and breath acetone for the model and the validation data; (b) Correlation between fat oxidation from the model and from the validation data.

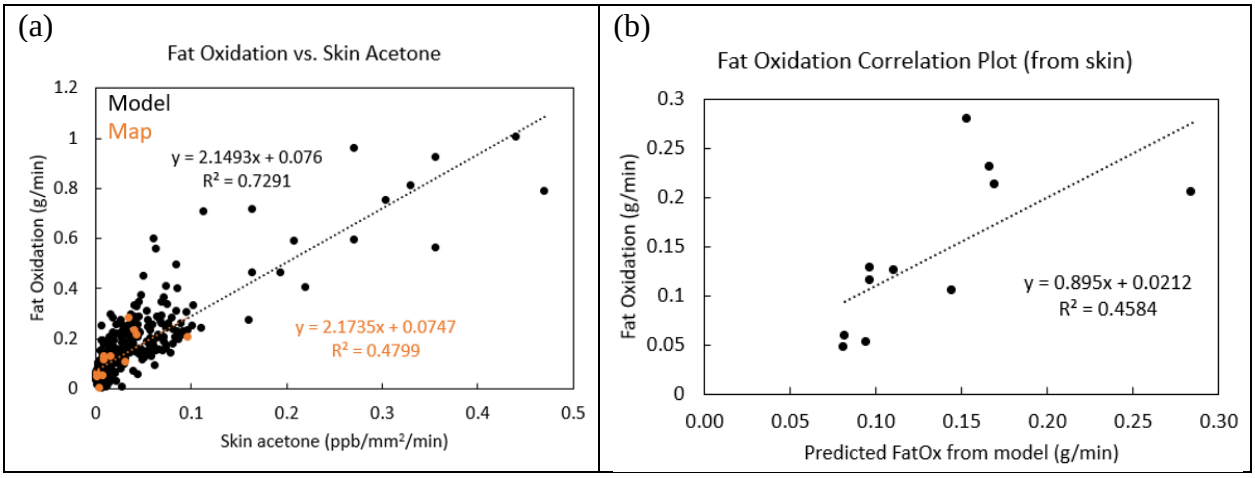

Figure S8. (a) Overlapping of the two correlations between fat oxidation and skin acetone for the model and the validation data; (b) Correlation between fat oxidation from the model and from the validation data.

5. Resting Energy Expenditure, Total Energy Expenditure and Energy Intake of the study's subjects

The tables below summarize the measurements of Resting Energy Expenditure (REE), estimations of Total Energy Expenditure (TEE), and the provided Energy Intake to the subjects of our study throughout the study for weeks 2 (w2), 4 (w4), 6 (w6) and 8 (w8).

Subject	Week	REE (kcal/day)	TEE (kcal/day)	Energy Intake (kcal/day)
1	W2	1373	1619	1619
	W4	1188	1400	1400
	W6	1263	1490	990
	W8	1177	1388	888
2	W2	1281	1632	1632
	W4	1320	1682	1682
	W6	1296	1651	1151
	W8	1287	1640	1140
3	W2	1607	1895	1895
	W4	1479	1743	1743
	W6	1507	1777	1277
	W8	1368	1613	1113
4	W2	1217	1435	1435
	W4	1227	1447	1447
	W6	1140	1344	844
	W8	1118	1319	819

Subject	Week	REE (kcal/day)	TEE (kcal/day)	Energy Intake (kcal/day)
5	W2	1058	1247	1247
	W4	1202	1417	1417
	W6	1280	1509	1009
	W8	1224	1443	943
6	W2	1458	1719	1719
	W4	1407	1659	1659
	W6	1320	1556	1056
	W8	1270	1497	997
7	W2	1142	1346	1346
	W4	1230	1451	1451
	W6	1153	1359	859
	W8	1065	1256	756
8	W2	1606	2046	2046
	W4	1702	2169	2169
	W6	1499	1910	1410
	W8	1572	2003	1503

Subject	Week	REE (kcal/day)	TEE (kcal/day)	Energy Intake (kcal/day)
9	W2	1365	1739	1739
	W4	1388	1768	1768
	W6	1386	1766	1266
	W8	1339	1705	1205
10	W2	2379	3031	3031
	W4	2400	3057	3057
	W6	2328	2966	2466
	W8	2367	3016	2516
11	W2	1521	1938	1938
	W4	1537	1959	1959
	W6	1674	2133	1633
	W8	1582	2015	1515
12	W2	1709	2177	2177
	W4	2122	2703	2703
	W6	2072	2640	2140
	W8	2061	2626	2126

Subject	Week	REE (kcal/day)	TEE (kcal/day)	Energy Intake (kcal/day)
13	W2	2126	2709	2709
	W4	2163	2756	2756
	W6	1959	2496	1996
	W8	2023	2578	2078
14	W2	1074	1266	1266
	W4	1064	1254	1254
	W6	1122	1322	822
	W8	970	1144	644
15	W2	1808	2304	2304
	W4	1717	2188	2188
	W6	1683	2145	1645
	W8	1734	2209	1709
16	W2	1628	2074	2074
	W4	1676	2135	2135
	W6	1584	2018	1518
	W8	1611	2052	1552

6. Revision of Gluconeogenesis Pathways

We consider the new ketogenesis-integrative model to be applicable under conditions of glycogenesis from glycerol and lactate with the rational and pathways summarized as follows[1, 2]:

1. Glycerol to Glucose: Glycerol is converted to glucose in the liver, and it is considered a relevant source of glucose at high ketogenesis conditions where hydrolysis of PSOG occurs to produce palmitate (reactions 8 to 10 in the main text).

Steps:

- **Glycerol to Glycerol-3-Phosphate:**
  - **Enzyme:** Glycerol kinase
  - **Reaction:** Glycerol + ATP → Glycerol-3-phosphate + ADP
- **Glycerol-3-Phosphate to Dihydroxyacetone Phosphate (DHAP):**
  - **Enzyme:** Glycerol-3-phosphate dehydrogenase
  - **Reaction:** Glycerol-3-phosphate + NAD+ → DHAP + NADH + H+
- **DHAP to Fructose-1,6-Bisphosphate:**
  - **Enzyme:** Aldolase (in glycolysis/gluconeogenesis pathway)
  - **Reaction:** DHAP + Glyceraldehyde-3-phosphate → Fructose-1,6-bisphosphate
- **Fructose-1,6-Bisphosphate to Fructose-6-Phosphate:**
  - **Enzyme:** Fructose-1,6-bisphosphatase
  - **Reaction:** Fructose-1,6-bisphosphate + H2O → Fructose-6-phosphate + Pi
- **Fructose-6-Phosphate to Glucose-6-Phosphate:**
  - **Enzyme:** Phosphohexose isomerase
  - **Reaction:** Fructose-6-phosphate ↔ Glucose-6-phosphate
- **Glucose-6-Phosphate to Glucose:**
  - **Enzyme:** Glucose-6-phosphatase
  - **Reaction:** Glucose-6-phosphate + H2O → Glucose + Pi

2. Lactate to Glucose: Lactate can be a potential source of glucose under exercise interventions, which are included in our study design. The Cori cycle describes the pathway of lactate produced by anaerobic glycolysis in muscles being converted to glucose in the liver.

Steps:

- **Lactate to Pyruvate:**
  - **Enzyme:** Lactate dehydrogenase
  - **Reaction:** Lactate + NAD+ → Pyruvate + NADH + H+
- **Pyruvate to Oxaloacetate:**
  - **Enzyme:** Pyruvate carboxylase
  - **Reaction:** Pyruvate + CO2 + ATP → Oxaloacetate + ADP + Pi
- **Oxaloacetate to Phosphoenolpyruvate (PEP):**
  - **Enzyme:** PEP carboxykinase
  - **Reaction:** Oxaloacetate + GTP → PEP + CO2 + GDP
- **PEP to 2-Phosphoglycerate to 3-Phosphoglycerate to 1,3-Bisphosphoglycerate to Glyceraldehyde-3-phosphate:**
  - **Enzymes:** Enolase, Phosphoglycerate mutase, Phosphoglycerate kinase, Glyceraldehyde-3-phosphate dehydrogenase
  - **Reaction Series:** These series of reactions reverse the glycolysis pathway
- **Glyceraldehyde-3-phosphate to Fructose-1,6-Bisphosphate:**

    - **Enzyme:** Aldolase
    - **Reaction:** Glyceraldehyde-3-phosphate + DHAP → Fructose-1,6-bisphosphate
- **Fructose-1,6-Bisphosphate to Fructose-6-Phosphate:**
    - **Enzyme:** Fructose-1,6-bisphosphatase
    - **Reaction:** Fructose-1,6-bisphosphate + H2O → Fructose-6-phosphate + Pi
- **Fructose-6-Phosphate to Glucose-6-Phosphate:**
    - **Enzyme:** Phosphohexose isomerase
    - **Reaction:** Fructose-6-phosphate ↔ Glucose-6-phosphate
- **Glucose-6-Phosphate to Glucose:**
    - **Enzyme:** Glucose-6-phosphatase
    - **Reaction:** Glucose-6-phosphate + H2O → Glucose + Pi

None of the gluconeogenesis pathways of glycerol and lactate include net VO_2, VCO_2, urea production or ketone production, affecting directly the mass balance of KIM model. However, increase of glucose availability due to gluconeogenesis of glycerol and lactate can be detected in KIM through the observation of an increased carb oxidation.

3. Glucogenic Amino Acids to Glucose: Glucogenic amino acids are converted to intermediates that enter the gluconeogenesis pathway. This route is prevalent in starvation conditions[2], which do not apply to our study design. Nevertheless, we describe this metabolic route below.

Common Glucogenic Amino Acids:

- **Alanine to Pyruvate:**
    - **Enzyme:** Alanine aminotransferase (ALT)
    - **Reaction:** Alanine + α-Ketoglutarate ↔ Pyruvate + Glutamate
- **Glutamine to Glutamate to α-Ketoglutarate:**
    - **Enzymes:** Glutaminase, Glutamate dehydrogenase
    - **Reaction:** Glutamine + H2O → Glutamate + NH3 (goes to urea cycle)
    - **Reaction:** Glutamate + NAD(P)+ + H2O → α-Ketoglutarate + NAD(P)H + H+ + NH3

Pathway: The resulting intermediates (pyruvate, oxaloacetate, α-ketoglutarate, succinyl-CoA, fumarate) enter the gluconeogenesis pathway.

Steps:

- **α-Ketoglutarate to Succinyl-CoA to Fumarate to Malate to Oxaloacetate:**
    - **Enzymes:** Various TCA cycle enzymes
    - **Reactions:** These intermediates proceed through the TCA cycle
- **Oxaloacetate to PEP:**
    - **Enzyme:** PEP carboxykinase
    - **Reaction:** Oxaloacetate + GTP → PEP + CO2 + GDP

- **PEP to 2-Phosphoglycerate to 3-Phosphoglycerate to 1,3-Bisphosphoglycerate to Glyceraldehyde-3-phosphate:**
    - **Enzymes:** Enolase, Phosphoglycerate mutase, Phosphoglycerate kinase, Glyceraldehyde-3-phosphate dehydrogenase
    - **Reaction Series:** These series of reactions reverse the glycolysis pathway
- **Glyceraldehyde-3-phosphate to Fructose-1,6-Bisphosphate:**
    - **Enzyme:** Aldolase
    - **Reaction:** Glyceraldehyde-3-phosphate + DHAP → Fructose-1,6-bisphosphate
- **Fructose-1,6-Bisphosphate to Fructose-6-Phosphate:**
    - **Enzyme:** Fructose-1,6-bisphosphatase
    - **Reaction:** Fructose-1,6-bisphosphate + H2O → Fructose-6-phosphate + Pi
- **Fructose-6-Phosphate to Glucose-6-Phosphate:**
    - **Enzyme:** Phosphohexose isomerase
    - **Reaction:** Fructose-6-phosphate ↔ Glucose-6-phosphate
- **Glucose-6-Phosphate to Glucose:**
    - **Enzyme:** Glucose-6-phosphatase
    - **Reaction:** Glucose-6-phosphate + H2O → Glucose + Pi

Considerations for future inclusion of gluconeogenesis from amino acids under ketogenesis with starvation conditions: The gluconeogenesis from amino acids requires ATP consumption, includes net exchange of protons, water, and CO_2, and produces urea. From all these elements, CO_2 affects the gas exchange, and therefore, a correction for VCO_2 should be applied under conditions where this metabolic route is prevalent. In addition, the nitrogen production rate from protein oxidation (*n*) calculated from urine urea excretion, should be corrected by the glycogenesis-produced (urea) nitrogen production.

References

(1) Salway, J. G. Blackwell Science. *Metabolism at a glance* **2000**, *2nd edition, Blackwell Science, foreword by D.K. Granner*, 73.
(2) Salway, J. G. Metabolism at a glance. *2nd edition, Blackwell Science, foreword by D.K. Granner* **2000**, *chart 20.1, Metabolism of amino acid to glucose in starvation*, 48-49.